

Proton Magnetic Relaxation in Gases

Robin L. Armstrong and Claude Lemaire

*Department of Physics
University of Toronto
Toronto, Canada, M5S 1A7*

Contents

I. Introduction	20
II. Measurement of Rotational Correlation Times	20
III. Measurement of Potential Energy Surfaces	21
IV. Dimers: The Effect of Creation and Annihilation Dynamics	23
V. Detailed Calculation of the τ_k in Terms of the Anisotropy Induced Splittings	26
VI. Conclusion	28
References	28

I. Introduction

Measurements of the longitudinal nuclear spin relaxation time, T_1 , in molecular gases are analogous to non-resonant absorption measurements; T_1 is determined primarily by that part of the spin-lattice interaction which couples free molecular states of the same energy. The contribution to T_1 of matrix elements of the spin-lattice interaction between rotational states of different energy is quenched.

II. Measurement of Rotational Correlation Times

Measurement of T_1 as a function of density through the region of the characteristic minimum provide values for various molecular parameters. It is now possible to obtain sufficiently accurate data in the vicinity of the T_1 minimum to see

the variation of the correlation times associated with different molecular rotational levels. As an illustration consider the proton T_1 data for hydrogen chloride. These data, shown in Figure 1, have been fit using a single relaxation time approximation (SRTA) and a multiple relaxation time approximation (MRTA). In the first case a common correlation time τ is assumed for all rotational levels; in the second case the distribution of correlation times τ_J is characterized by an average value $\tau_0 = (\Gamma_0)^{-1}$ and a dispersion parameter $\beta = \Delta\Gamma/\Gamma_0$ where formal expressions relating τ_0 and β to the τ_J values exist.

The solid line through the data represents the best MRTA fit; for this fit $\beta_{HCl} = 0.298 \pm 0.015$. Figure 2 shows the differences between the T_1 data and the best SRTA and MRTA fits. It is clear that the MRTA fit is significantly better. One can probe the variation of the correlation times associated with different rotational levels.

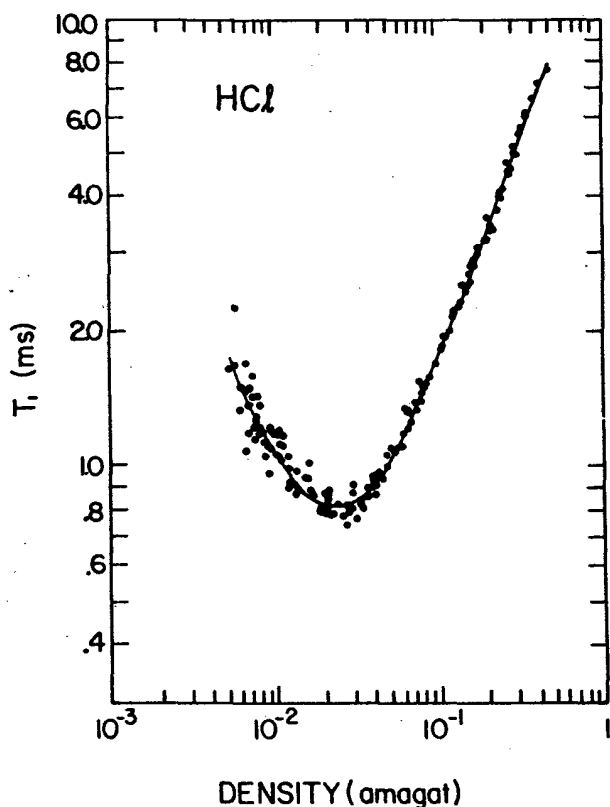


Figure 1. The density dependence of the proton relaxation time through the region of the characteristic minimum for hydrogen chloride.

III. Measurement of Potential Energy Surfaces

Measurements of the temperature variation of T_1/ρ taken in the extreme narrowing, binary collision regime in a molecular gas M infinitely dilute in an inert gas X should provide a significant test of the anisotropic part of any proposed M-X intermolecular potential energy surface. To make the connection with this surface, it is necessary to express T_1 in terms of quantities that may be directly calculated once an intermolecular potential energy surface has been supplied. To accomplish this goal, one may use the projection operator formalism to obtain a "memory equation" for that part of the distribution function density ma-

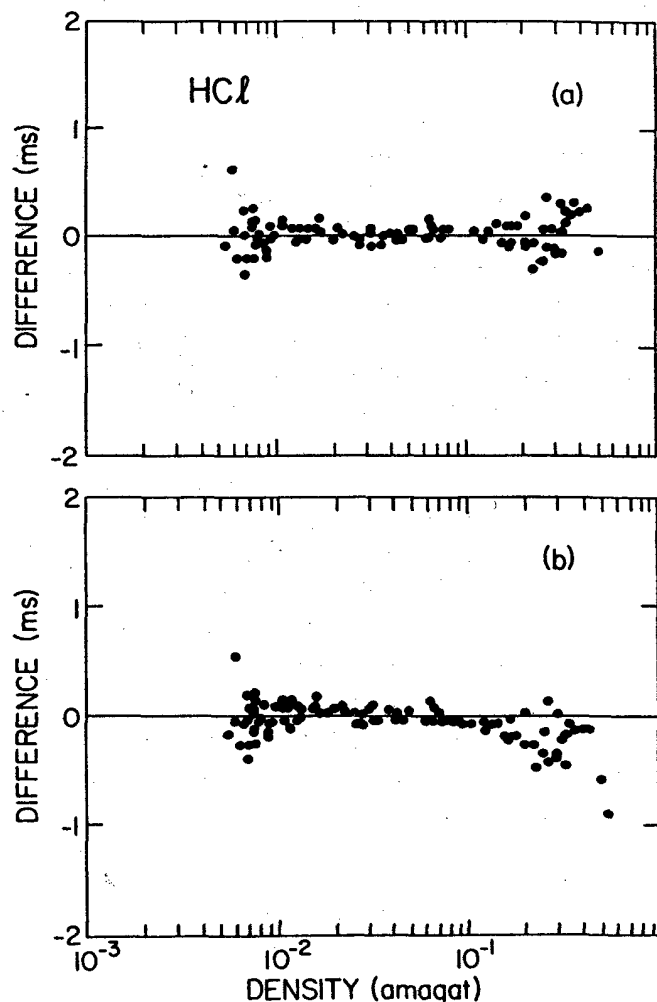


Figure 2. The differences between the T_1 data in hydrogen chloride and (a) the best SRTA fit; (b) the best MRTA fit.

trix characterizing the gaseous system and proportional to the nuclear spin operator I . One can then deduce an integral equation governing the time dependence of the non-equilibrium part of the nuclear magnetization in terms of a kernel having the form of an autocorrelation function. The required connection is thereby made.

Until recently the $T_1/\rho)_{lin}$ data available were not sufficiently reliable to provide meaningful tests of intermolecular potential energy surfaces. Recent data taken in H_2 -He mixtures were improved partly by using a phase alternation inversion recovery (PAIR) pulse sequence to eliminate the effects of various pulse imperfections and by maintaining tight control on the coil and transmitter tuning and on the pulse length and resonance frequency settings. In this way T_1 data reproducible to within 2% over a period of many months have been obtained. However, what was more important, the experimental data were taken on mixtures with 2% and 10% H_2 in He. This choice of mixtures, both quite dilute in H_2 , has several advantages: (1) The need for a nonlinear extrapolation of $T_1/\rho)_{lin}$ as a function of concentration to the infinitely dilute limit is eliminated; (2) The extrapolation does not require the mixture virial coefficients; a linear extrapolation of T_1/ρ as a function of concentration followed by a conversion of the pressure P to a density ρ using the second virial coefficient of He is sufficient.

The proton $T_1/\rho)_{lin}$ data taken over the temperature range 90 to 300 K are shown in Figure 3.

Note that the values obtained directly from the 2% mixture differ from the infinitely dilute values $T_1/\rho)_{lin}^\infty$ by only about 3%. The $T_1/\rho)_{lin}^\infty$ data are shown along with previously reported data in Figure 4. Note that the old data show more scatter and are systematically higher than the present data. The figure also shows predictions calculated from four theoretical potentials labelled SG, MVAW, RS and KS. It is clear that: (1) The data are quite capable of distinguishing between the various surfaces; (2) Only the KS potential surface is able to account for the data and this ab initio potential does so in a very convincing manner.

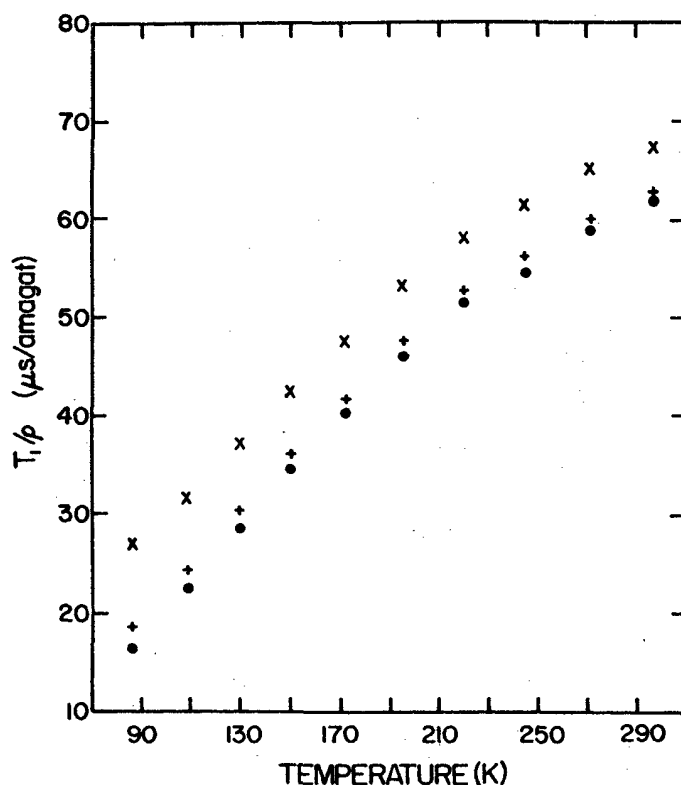


Figure 3. $T_1/\rho)_{lin}$ data taken over the temperature range 90 to 300 K for H_2 -He mixtures with 10% H_2 (x) and 2% H_2 (+). The infinitely dilute values $T_1/\rho)_{lin}^\infty$ obtained by linear extrapolation are also shown (•).

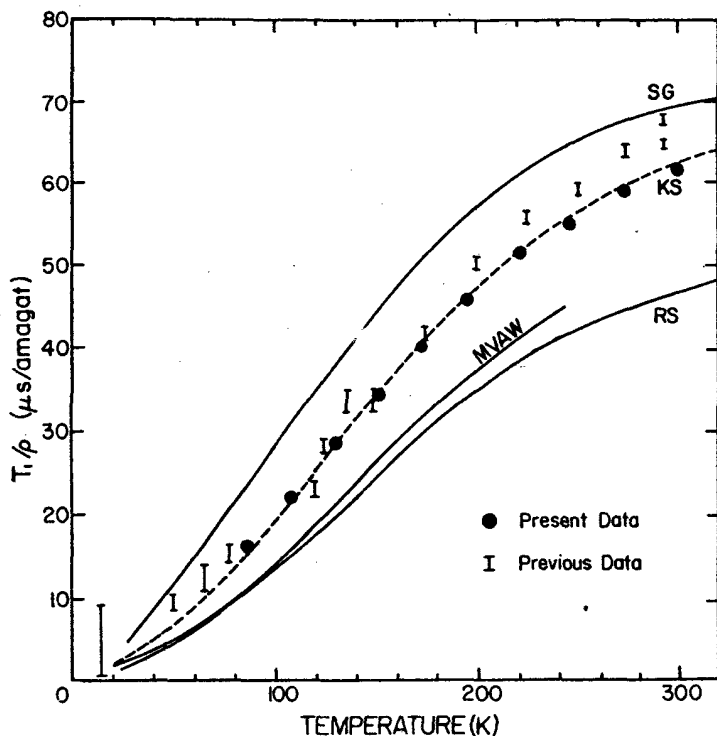


Figure 4. A comparison of $T_1/\rho)_{lin}^\infty$ data with predictions based on several theoretical potentials. Note the excellent agreement between the present data the prediction (KS) based on the most recent theoretical potential by Kohler and Schaefer.

IV. Dimers: The Effect of Creation and Annihilation Dynamics

For purely binary collisions and in the extreme narrowing regime, T_1/ρ is a constant. Figure 5 shows plots of $T_1/\rho)_{lin}$ vs ρ for H_2 -He and H_2 -Ar mixtures. In the former case T_1/ρ is independent of ρ ; in the latter case it is not. One must conclude that the result in H_2 -Ar is a consequence of a multiple collision process. Indeed such is the case; the specific cause has been identified and the effect calculated from first principles. The two obvious clues provided by the data are: (1) The effect occurs in an H_2 -Ar mixture but not in an H_2 -He mixture; (2) The effect has a characteristic density dependence as it is not present at either low densities or high densities and goes through a maximum at a particular density.

The observed non-linear density dependence of T_1 results from the creation-annihilation dynamics of H_2 -Ar dimers. In the H_2 -He mixture the van der Waals interaction is not sufficiently strong to

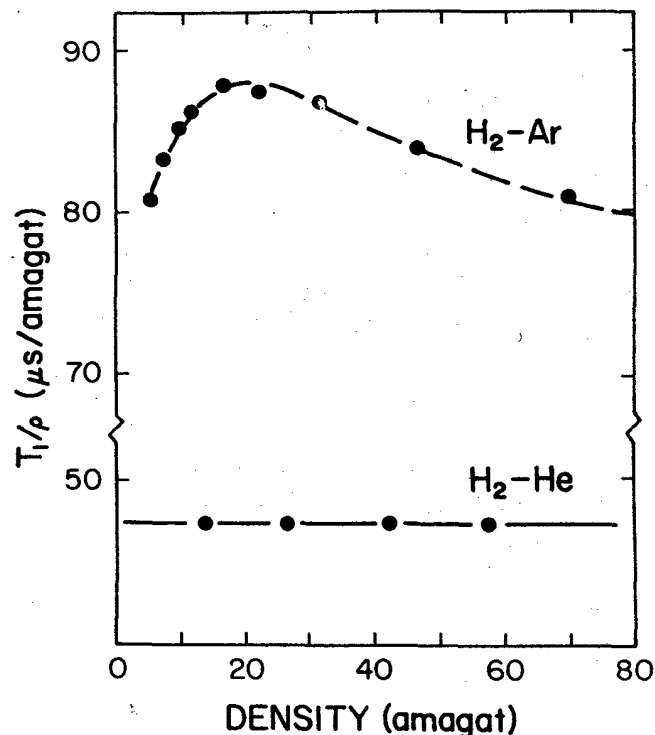


Figure 5. Plots of T_1/ρ as a function of density ρ for H_2 -He and H_2 -Ar mixtures.

sustain bound states of an H₂-He dimer; in contrast, the H₂-Ar system can sustain bound states characterized by rotational angular momentum L . The H₂-Ar dimer has rotational constants

$$B = 0.562 \text{ cm}^{-1}; D_L = 5.0 \times 10^{-4} \text{ cm}^{-1}.$$

To a good approximation the H₂ molecule retains its integrity while participating in such a bound state. At low densities there are too few dimers present in the mixture to affect the proton spin relaxation; at high densities the dimer lifetime is too short for the existence of the dimers to affect the proton spin relaxation.

It is the anisotropy induced splitting of the rotational states of the dimer that results in their contribution to the proton relaxation. These splittings are indicated in Figure 6 for the $J = 1$ rotational state of the H₂ molecule. No actual transitions occur among the rotational substates, but rather a dephasing of the rotational coherence occurs. This dephasing results in a reduction of the correlation times that describe the rotational polarizations. The couplings between the nuclear spins, the molecular rotations and the other degrees of freedom may be described schematically as in Figure 7. The coupling of the rotational polarizations to the nuclear spins is given by the hamiltonian

$$H_{sl} = \omega_{(k)} \mathbf{I}^{(k)} O^{(k)} \mathbf{J}^{(k)}.$$

The index k takes two values: $k = 1$ for the spin-rotation interaction and $k = 2$ for the spin-spin dipolar interaction. In the SRTA approximation each correlation function $\langle J^{(k)}(0) J^{(k)}(t) \rangle$ is characterized by just one correlation time τ_k .

In the motional narrowing limit the relaxation rates $(T_{1k})^{-1}$ are proportional to the correlation times τ_k . The relaxation rates for $k = 1, 2$ are additive. It remains to calculate τ_k in terms of the anisotropy induced splittings. The result is

$$\begin{aligned} 1/\tau_k &= \sum_L \sum_{jj'} C_k(Ljj') J(\omega_{jj'}) \\ &= \sum_L \sum_{jj'} C_k(Ljj') \frac{1}{T_f} \frac{\omega_{jj'}^2 \tau^2}{1 + \omega_{jj'}^2 \tau^2} \end{aligned}$$

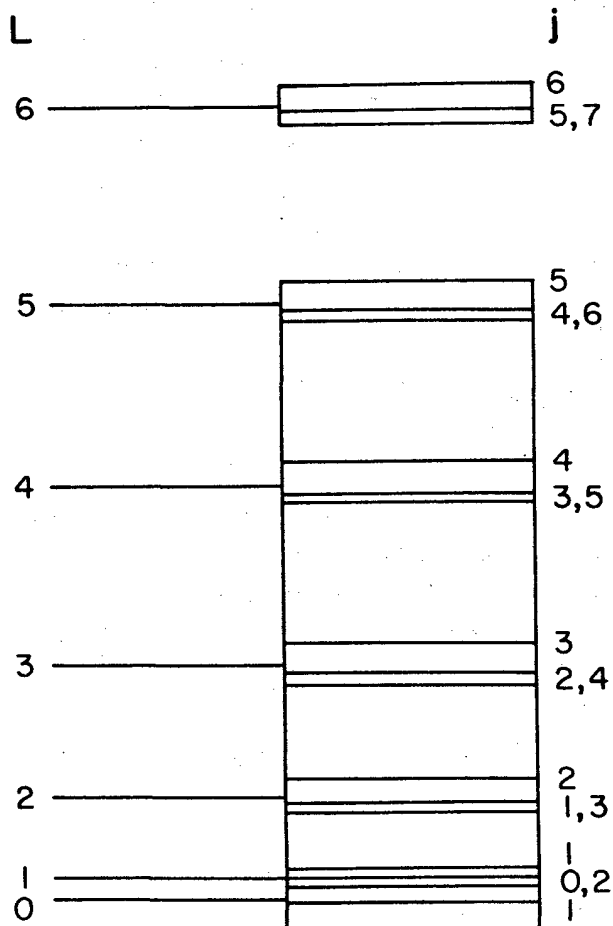


Figure 6. Anisotropy induced splitting of the rotational states of the H₂-Ar dimer for the $J = 1$ rotational state of the H₂ molecule. The total angular momentum j is given by $j = L + J$.

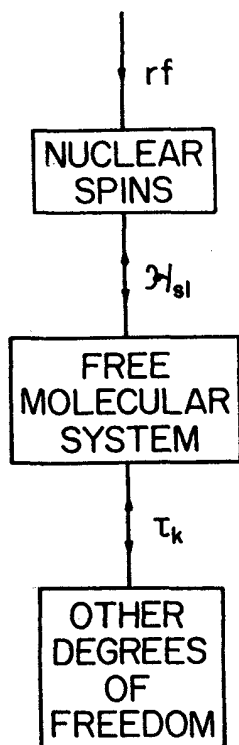


Figure 7. Schematic illustration of the couplings between the nuclear spins, the molecular rotations and the other degrees of freedom.

where T_f^{-1} is the formation rate of the dimers, τ^{-1} is the annihilation rate of the dimers, $J(\omega_{jj'})$ is the spectral density with $\omega_{jj'}$ the anisotropy induced splittings and the $C_k(Ljj')$ are temperature dependent weighting factors.

The thermal equilibrium rate equation is

$$\frac{[H_2 - Ar]}{\tau} = \frac{[H_2]}{T_f}$$

where the brackets [] indicate the respective concentrations of the molecular species and the equilibrium constant K is

$$K = \frac{[H_2 - Ar]}{[Ar][H_2]}$$

From these equations it follows that

$$\frac{\tau}{T_f} = [Ar]K.$$

But from the thermodynamics for the chemical equilibrium of an ideal gas mixture,

$$K = V \frac{Q(H_2 - Ar)}{Q(Ar)Q(H_2)}$$

where V is the volume of the sample and the Q 's are the respective atomic and molecular partition functions. It follows that

$$K = CT^{-3/2} \exp(D_0/kT) Q_{rot}$$

with

$$C = (h^2/2\pi\mu k)^{3/2},$$

$$Q_{rot}(H_2 - Ar) = \sum_{L=0}^{\infty} (2L+1) \exp[-E(L)/kT].$$

$$E(L) = BL(L+1) - D_L L^2(L+1)^2.$$

In the above expressions μ is the reduced mass of the H_2 -Ar pair, D_0 is the dissociation energy of the ground state of the H_2 -Ar dimer and T is the temperature. From simple kinetic theory

$$\frac{1}{\tau} = \rho \langle \nu \rangle \sigma$$

with σ the annihilation cross-section and $\langle \nu \rangle$ the mean relative speed of the colliding pair. Therefore

$$\frac{1}{T_f} = K \rho^2 \langle \nu \rangle \sigma.$$

Note that the formation rate is proportional to the square of the density as expected for a three-body process. In the low density limit

$$\omega_{jj'}\tau \gg 1 \text{ and } J(\omega_{jj'}) = 1/T_f$$

from which it follows that T_1/ρ is proportional to ρ . In the high density limit

$$\omega_{jj'}\tau \ll 1 \text{ and } J(\omega_{jj'}) = \frac{\omega_{jj'}^2 K}{\langle \nu \rangle \sigma}$$

so that T_1/ρ is proportional to $1/\rho$. A maximum in T_1/ρ occurs at density ρ_{max} for which

$$\omega_{jj'} = 1.$$

Hence

$$\rho_{max} = \frac{\omega_{jj'}}{\nu \sigma} \cong 15 \text{ amagat.}$$

A comparison of the theory with experimental data taken at $T = 160 \text{ K}$ is shown in Figure 8. The annihilation cross-section σ and the equilibrium constant K are taken as adjustable parameters. The annihilation cross-section is of the order of the geometric cross-section which implies that the dimer lifetime is approximately the collision time. The equilibrium constant is about one-half that predicted from equilibrium thermodynamics which may suggest that the dimer population is not thermalized.

V. Detailed Calculation of the τ_k in Terms of the Anisotropy Induced Splittings

The anisotropic van der Waals potential

$$H_1 = V_2(R)P_2(\cos \Theta)$$

in general induces transitions between the various levels (L, J) of the dimer. The selection rules for these transitions are

$$\Delta L = 0, \pm 2; \Delta J = 0, \pm 2; \Delta j = 0.$$

However, below 200 K it is sufficient to consider only the $J = 1$ rotational level of the H_2 molecule and therefore $\Delta j, \Delta J$ and ΔL must all be 0 so that

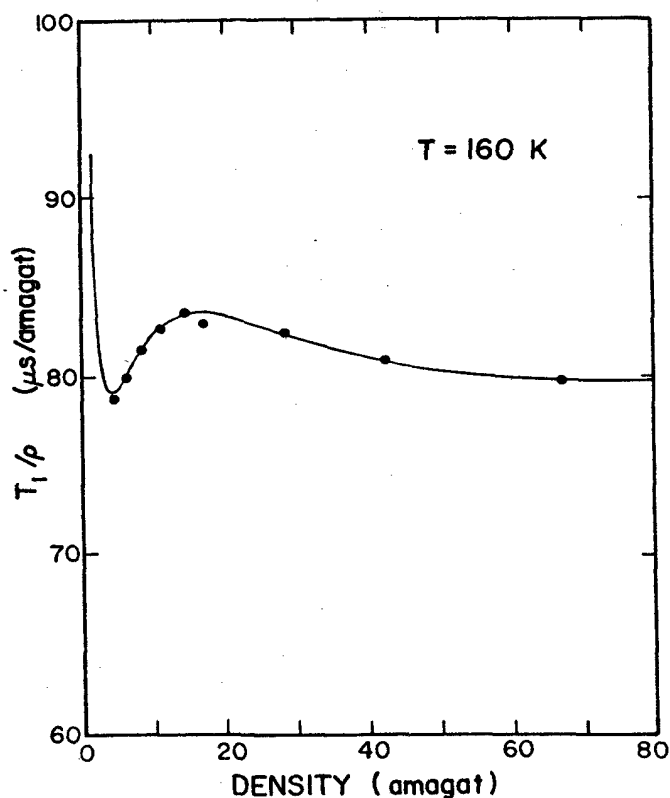


Figure 8. The anomalous density dependence of T_1/ρ in an H_2 -Ar mixture at 160 K as accounted for by the creation-annihilation dynamics of H_2 -Ar dimers.

no transitions occur between (L, J) manifolds and each manifold may be treated independently.

Assume that a dimer is formed at $t = 0$. The density matrix $\rho(0)$ at time $t = 0$ is

$$\rho(0) = \sum_L \rho(L; 0) \otimes \rho(J; 0)$$

where

$$\rho(L; 0) = \{\exp[-E(L)/kT]/Q\} \Pi_L.$$

The $\rho(J; 0)$ can be expressed in terms of irreducible tensor operators $T(J)_{kq}$ as

$$\rho(J; 0) = \sum_{kq} \langle T^\dagger(J)_{kq} \rangle T(J)_{kq}$$

where

$$T(J)_{00} = (2J + 1)^{1/2} \Pi$$

$$T(J)_{1q} = [3/J^2(2J + 1)]^{1/2} J_q$$

$$T(J)_{2q} = [30/J^2(4J^2 - 3)(2J + 1)]^{1/2} J_q^{(2)}$$

with J_q and $J_q^{(2)}$ the spherical components of the irreducible tensors \mathbf{J} and $\mathbf{J}^{(2)}$. The coefficients $\langle T^\dagger(J)_{kq} \rangle$ specify the amounts of \mathbf{J} and $\mathbf{J}^{(2)}$ polarizations present at $t = 0$. Therefore

$$\rho(0) = \sum_L \sum_{kq} \{\exp[-E(L)/kT]/Q\} \times$$

$$\langle T^\dagger(J)_{kq} \rangle [\Pi_L \otimes T(J)_{kq}].$$

The density matrix $\rho(t)$ at time t is

$$\rho(t)U(t)\rho(0)U^\dagger(t)$$

$$= \sum_L \sum_{kq} \{\exp[-E(L)/kT]/Q\} \langle T^\dagger(J)_{kq} \rangle U(t) \times$$

$$[\Pi_L \otimes T(J)_{kq}] U(t).$$

For the present purposes only $\rho(J, t)$ is required and it can be expanded as

$$\rho(J, t) = \sum_{kq} \langle T^\dagger(J)_{kq} \rangle T(J)_{kq} \langle \cdot \rangle$$

The coefficients $\langle T^\dagger(J)_{kq} \rangle$ which describe the rotational state at time t are given by

$$\langle T^\dagger(J)_{kq} \rangle = \text{tr}[\rho(J, t) T^\dagger(J)_{kq}]$$

$$= \text{tr}[\rho(t) \Pi \otimes T^\dagger(J)_{kq}]$$

$$= \sum_L P_L \sum_{kq} \langle T^\dagger(J)_{k'q'} \rangle G^L(J, t)_{qq', kk'}$$

where

$$P_L = (2L + 1) \exp[-E(L)/kT]/Q$$

and

$$G^L(J, t)_{qq', kk'} =$$

$$\text{tr}\{U(t) [\Pi_L \otimes T(J)_{k'q'}] U^\dagger(t) \times$$

$$[\Pi_L \otimes T^\dagger(J)_{kq}]\} / 2L + 1.$$

Since $U(t)$ is diagonal in the eigenstate representation $|(LJ)jm\rangle$, polarizations with different ranks and components are not mixed by the interaction. As a result

$$G^L(J, t)_{qq', kk'} = G^L(J, t)_k \delta_{kk'} \delta_{qq'} =$$

$$\sum_{jj'} \frac{(2j' + 1)(2j + 1)}{(2L + 1)} \begin{bmatrix} J & j' & L \\ j & J & k \end{bmatrix}^2 \cos[(E_j - E_{j'})t/\hbar]$$

Therefore

$$\langle T^\dagger(J)_{kq} \rangle = \sum_L P_L G^L(J, t)_k \langle T^\dagger(J)_{kq} \rangle.$$

Finally, it is necessary to consider the calculation of $\rho_H(t)$, the density matrix of the H_2 molecules in the presence of the dimers. There are two contributions: (1) that due to free molecules for which there is no evolution of $\rho_H(t)$; (2) that due to bound molecules for which the evolution of $\rho_H(t)$ is by the action of the intermolecular potential as described above.

A coarse grained approximation can be applied to relate $\rho_H(t)$ to $\rho_H(t + \Delta t)$ where Δt is large enough so that many dimers are formed and annihilated in the interval *but* Δt is still much smaller than the average time between dimer formations, T_f . One can write

$$\rho_H(t + \Delta t) = (1 - \Delta t/T_f) \rho_H(t)$$

$$+ (\Delta t/T_f) \langle \rho(J, \xi, t) \rangle_{AV}$$

where $(1 - \Delta t/T_f)$ is the fraction of H_2 molecules that remain free and $(\Delta t/T_f)$ the fraction that participate in a bound state during the interval Δt . The quantity ξ appearing in $\langle \rho(J, \xi, t) \rangle$ is a stochastic variable representing the dimer lifetime and the average is over this variable. Setting

$$\rho_H(t) = \rho(J, \xi = 0, t)$$

implies that $G^L(J, \xi = 0, t)_k = 1$ and therefore that

$$\langle T^\dagger(J, 0, t)_{kq} \rangle = \langle T^\dagger(J)_{kq} \rangle$$

It follows that

$$\begin{aligned} \langle T^\dagger(J, \xi, t)_{kq} \rangle &= \langle T^\dagger(J)_{kq} \rangle \\ &+ \sum_L P_L [G^L(J, \xi, t)_k - 1] \langle T^\dagger(J)_{kq} \rangle. \end{aligned}$$

Hence

$$\frac{d}{dt} \langle T^\dagger(J)_{kq} \rangle = -\frac{1}{\tau_k} \langle T^\dagger(J, t)_{kq} \rangle$$

with

$$1/\tau_k = \frac{1}{T_f} \sum_L P_L \langle 1 - G_k^L \rangle_{AV}.$$

Assuming that ξ is governed by an exponential law of probability given by $P(t|\xi)t + dt = \exp(-t/\tau)dt/\tau$ then

$$\langle 1 - G_k^L \rangle_{AV} = 2 \sum_{jj'} \frac{(2j' + 1)(2j + 1)}{(2L + 1)} \times$$

$$\left[\begin{matrix} J & j' & L \\ j & J & k \end{matrix} \right]^2 \langle \sin^2(\omega_{jj'}\xi/2) \rangle_{AV}$$

$$= \sum_{jj'} \frac{(2j' + 1)(2j + 1)}{(2L + 1)} \left[\begin{matrix} J & j' & L \\ j & J & k \end{matrix} \right]^2 \frac{(\omega_{jj'}\tau)^2}{[1 + (\omega_{jj'}\tau)^2]}$$

with

$$\omega_{jj'} = (E_j - E_{j'})/\hbar.$$

It follows that

$$\frac{1}{\tau_k} = \sum_L \sum_{jj'} C_k(Ljj') \frac{1}{T_f} \frac{(\omega_{jj'}\tau)^2}{[1 + (\omega_{jj'}\tau)^2]}$$

with

$$C_k(Ljj') = \frac{\exp[-E(L)/kT]}{Q} \times$$

$$(2j' + 1)(2j + 1) \left[\begin{matrix} J & j' & L \\ j & J & k \end{matrix} \right]^2.$$

VI. Conclusion

This review has described three quite different molecular physics experiments all utilizing proton T_1/ρ measurements. The first experiment demonstrated that it is now possible to carry out measurements in molecular gases in the vicinity of the characteristic T_1 minimum with sufficient accuracy to permit studies of the variation of the correlation time τ_J with the molecular rotational level J . Data for hydrogen chloride were presented. The second experiment illustrated that measurements taken in the extreme narrowing, binary collision regime provide a powerful test of the anisotropic part of the H_2 -noble gas potential energy surfaces. Data taken in H_2 -He mixtures have been used in a very successful test of an ab initio potential. The third experiment showed a new effect resulting from the presence of dimers in H_2 -noble gas mixtures. Measurements in the 10 to 30 amagat range in H_2 -Ar mixtures have exhibited anomalous behavior. A theory has been outlined which explains the effect as a consequence of the creation and annihilation of H_2 -Ar dimers.

VII. References

- ¹C. Lemaire and R. L. Armstrong, *J. Chem Phys.* **81** 1626-1631 (1984).
- ²C. Lemaire, R. L. Armstrong and F. R. McCourt, *J. Chem Phys.* **81** 5275-5280 (1984).
- ³C. Lemaire and R. L. Armstrong, *Can J. Phys.* **63** 179-187 (1985) and references contained therein.